JOURNAL OF CATALYSIS 113, 517–524 (1988)

Kinetics of the Oxidative Coupling of Methane over 1 wt% Sr/La_2O_3

JEFFREY M. DEBOY AND ROBERT F. HICKS[1]

W. R. Grace & Company, Research Division, Columbia, Maryland 21044

Received February 8, 1988; revised May 16, 1988

The reaction network has been determined for the oxidative coupling of methane over 1 wt% Sr/La_2O_3 by varying the residence time at a fixed feed composition of 0.46 atm CH_4, 0.045 atm O_2, and 0.50 atm argon. Ethane and CO are the primary products of methane reaction. Ethylene is formed from ethane, while CO_2 appears to form from CO. The preexponential factors and apparent activation energies, obtained in the interval from 700 to 750°C, are $A_{CH_4} = 4.7 \times 10^8$ (moles CH_4 consumed/g hr), $E_{CH_4} = 39.4$ (kcal/mole); $A_{C_2H_6} = 8.5 \times 10^7$ (moles C_2H_6 produced/g hr), $E_{C_2H_6} = 36.8$ (kcal/mole); and $A_{CO_x} = 13{,}600$ (moles CO + CO_2 produced/g hr), $E_{CO_x} = 23.9$ (kcal/mole). Substantial amounts of hydrogen are produced during the oxidative coupling of methane. The distribution of CO, CO_2, H_2, and H_2O in the product is controlled by the water gas shift equilibrium.

INTRODUCTION

The current abundance of natural gas has spurred much research on new catalytic processes for converting methane into more valuable and more easily transportable organic compounds (*1, 2*). A promising new catalytic reaction is the oxidative coupling of methane. Methane and oxygen are fed either sequentially (*3–7*) or together (*8–35*) over a solid metal oxide at temperatures between 600 and 1000°C and are converted into a mixture of ethane, ethylene, carbon oxides, hydrogen, and water. Provided the yield of ethylene is made high enough, oxidative coupling of methane can be combined with ethylene oligomerization to provide an economic route to liquid fuels from natural gas.

Previous studies found that when methane and oxygen are fed simultaneously, the selective catalysts are supported Pb, Sn, and Bi oxides (*8–13*), alkaline earth oxides (*14–21*), rare earth oxides, excluding CeO_2 and Pr_6O_{11} (*21–27*), and alkali-promoted metal oxides (*14–19, 21, 28–34*). The highest activities are observed for the rare earth oxides. We have shown that many of the effective catalysts are chemically similar (*21*): They are solid bases, exhibiting one stable oxidation state, and strongly adsorb CO_2 and H_2O from the atmosphere. The basic surface promotes hydrogen atom abstraction from the methane with subsequent coupling of CH_3 to form ethane. Conversely, multiple oxidation states of the metal promote complete oxidation of the methane through a redox reaction mechanism.

Among the many possible combinations of oxides that catalyze the oxidative coupling of methane, La_2O_3 promoted with Sr exhibits high activity and good selectivity (*21, 35*). In order to gain further insight into this catalytic system, the reaction kinetics were determined in a fixed bed, operating under differential conversion of methane and oxygen. Herein we report the results of our kinetic study.

METHODS

Lanthanum oxide of 99.99% purity was obtained from Union Molycorp. Strontium nitrate (Aldrich Chemical Co.) was deposited onto La_2O_3 by incipient wetness impregnation. The catalyst was dried in a vacuum for 12 h at 110°C, calcined for 4 hr at

[1] Present address: UCLA Chemical Engineering Department, 5531 Boelter Hall, Los Angeles, CA 90024.

0021-9517/88 $3.00

600°C, pelletized to 32–50 mesh size, and stored in a desiccator. The finished catalyst contained 1 wt% Sr metal, and it had a surface area of 3 m^2/g.

The reaction kinetics were obtained in a standard fixed bed reactor. A catalyst bed from 1.6 to 6.4 mm deep was suspended in a 4-mm-i.d. quartz tube. The tube was immersed in a fluidized sand bath heater for temperature control. The temperature was measured along the quartz wall. Separate measurements showed that the bed inlet temperature and the quartz wall temperature differed by a constant amount of about 20°C. The results described below are reported using the wall temperature. Methane, oxygen, and argon were fed to the reactor using mass flow controllers at pressures slightly above 1 atm. The composition of the reactor exit stream was measured by on-line gas chromatography. A 6-ft nickel column of Gas Chrome 220 (Alltech) attached to an FID was used for analysis of the hydrocarbons, while a 6-ft stainless-steel column of Carbosphere (Alltech) attached to a TCD was used for analysis of the inorganic gases.

During operation the catalyst rapidly attained a steady-state activity which remained constant over 48 hr. Kinetic measurements were made between 0.5 and 48 hr of reaction.

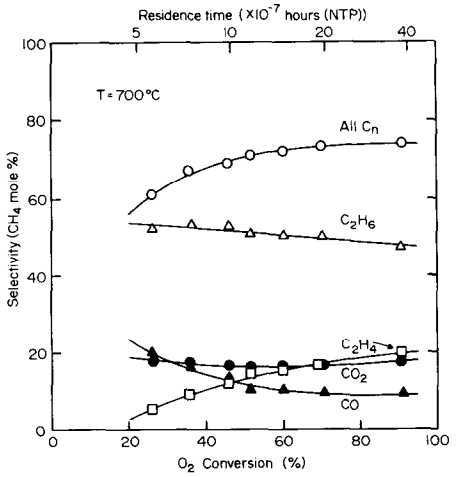

FIG. 1. The dependence of the product selectivity upon oxygen conversion and residence time at 700°C.

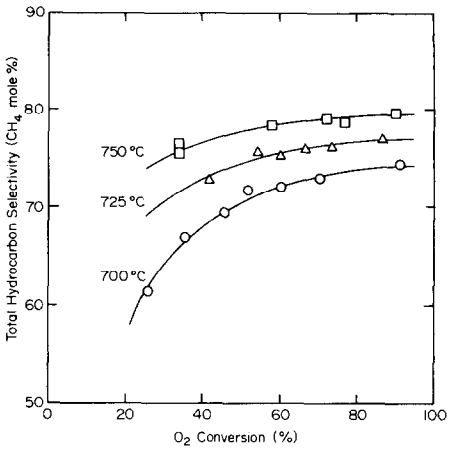

FIG. 2. The dependence of the total hydrocarbon selectivity upon oxygen conversion and temperature.

RESULTS

A series of measurements in which the flow rate over the catalyst was varied at a constant feed composition of 45.5% CH_4, 4.5% O_2, and 50% argon was made. In this way, the intrinsic rates of reaction could be determined by monitoring the amount of product formed as a function of residence time. These results are summarized in Figs. 1–9.

Figure 1 shows how the product selectivity varied with the residence time and amount of oxygen converted. Over the eightfold variation in contact time, the selectivities to ethane and CO_2 are nearly constant, the selectivity to CO declines, and the selectivities to ethylene and all coupled hydrocarbons (all C_n) increase. These trends were also observed at reaction temperatures of 725 and 750°C, except that the hydrocarbon selectivities are displaced upward relative to CO and CO_2 with increasing temperature. The effect of temperature on the total hydrocarbon selectivity is shown in Fig. 2.

The dependence of methane conversion on residence time is plotted in Fig. 3. At short residence times the data fall on

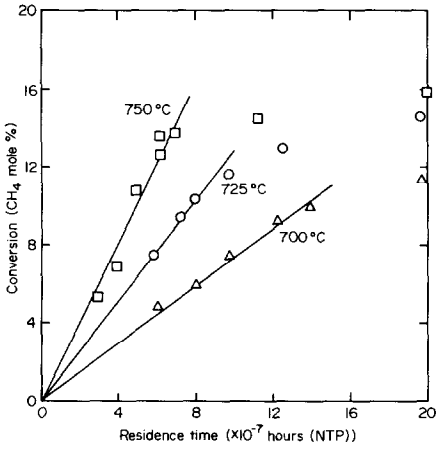

FIG. 3. The dependence of methane conversion upon residence time and temperature.

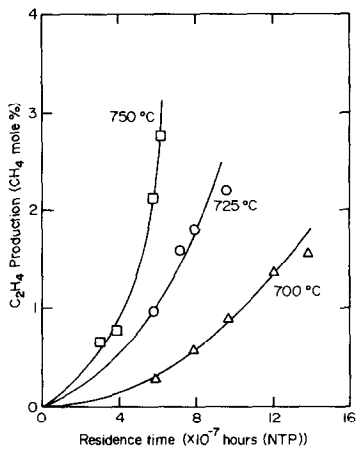

FIG. 5. The dependence of ethylene production upon residence time and temperature.

straight lines that intersect the origin. The rates at each temperature have been computed from the slopes of the lines, and then used to construct an Arrhenius relationship. The preexponential factor and apparent activation energy for the rate of methane reaction are

$$A_{CH_4} = 4.7 \times 10^8 \quad \text{(moles } CH_4\text{/g hr)}$$

$$E_{CH_4} = 39.4 \pm 0.1 \quad \text{(kcal/mole)}$$

(1 kcal = 4.184 kJ).

The dependence of the ethane production on residence time is shown in Fig. 4. The ethylene production is also included, since it is produced in series from ethane. The slopes of the lines at each temperature give the rates of ethane formation. From these values the preexpoential factor and apparent activation energy are calculated to be

$$A_{C_2H_6} = 8.5 \times 10^7 \quad \text{(moles } C_2H_6\text{/g hr)}$$

$$E_{C_2H_6} = 36.8 \pm 0.1 \quad \text{(kcal/mole)}.$$

The dependencies of the C_2H_4, CO, and CO_2 production on residence time are shown in Figs. 5, 6, and 7, respectively. The upward curving lines observed for ethylene formation indicate that it is a second-

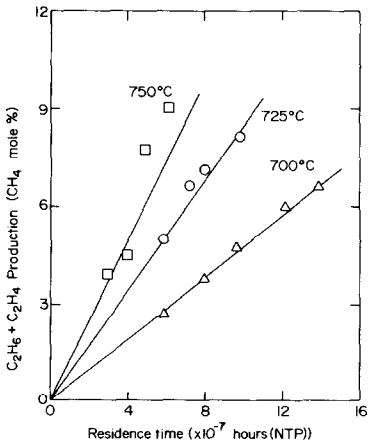

FIG. 4. The dependence of ethane production upon residence time and temperature.

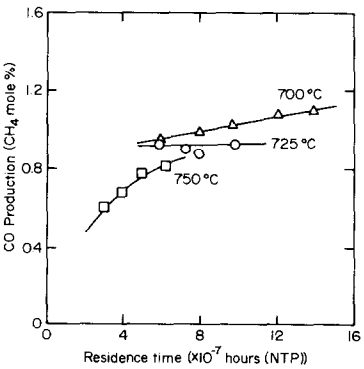

FIG. 6. The dependence of carbon monoxide production upon residence time and temperature.

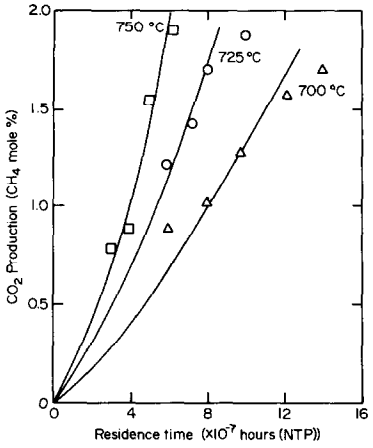

FIG. 7. The dependence of carbon dioxide production upon residence time and temperature.

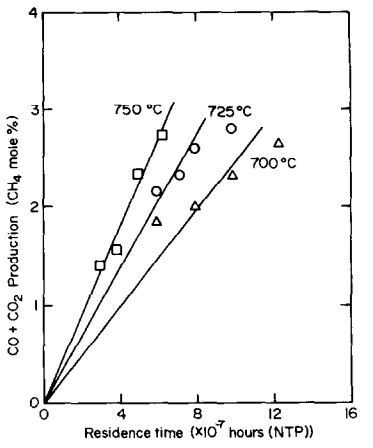

FIG. 8. The dependence of carbon monoxide and carbon dioxide production upon residence time and temperature.

ary reaction product, formed from the dehydrogenation of ethane. The amount of CO produced shows a weak dependence on residence time which does not extrapolate back to the origin. Such a relationship suggests that the CO may be a primary reaction product but is rapidly consumed in a further reaction or is influenced by a fast equilibrium with other products. The upward curving lines observed for CO_2 formation in Fig. 7 indicate that CO_2 is formed in a secondary reaction, probably by the oxidation of CO. In Fig. 8 the combined rates of CO and CO_2 production are plotted as a function of residence time. The relationship appears to be linear, from which the preexponential factor and apparent activation energy are calculated to be

$$A_{CO_x} = 13{,}600 \quad \text{(mole CO + } CO_2\text{/g hr)}$$

$$E_{CO_x} = 23.9 \pm 0.1 \quad \text{(kcal/mole)}.$$

Throughout all of the measurements described above, the moles of methane consumed maintained a fixed multiple of 1.65 times the moles of oxygen consumed. Thus, the reaction stoichiometry for methane and oxygen consumption is unaffected by the moderate shift in product distribution that occurs with changes in contact time and temperature.

The oxidative coupling of methane produces substantial amounts of hydrogen. As shown in Fig. 9, carbon monoxide and hydrogen maintain a constant fixed ratio of $CO/H_2 = 0.54$ over the variation in residence times and temperatures studied. These data indicate that CO and H_2 are generated in the same reaction or are related through a rapid chemical equilibrium. The most likely explanation is that the CO and H_2 are fixed relative to one another through the water gas shift equilibrium.

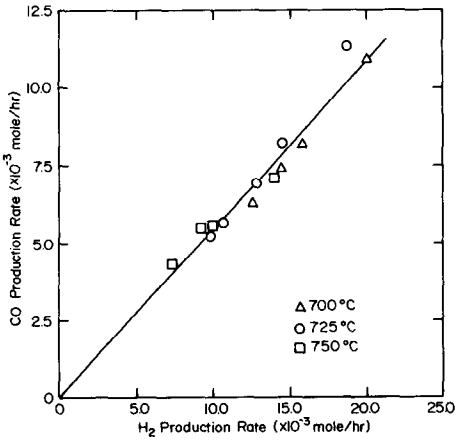

FIG. 9. The relationship between hydrogen and carbon monoxide production rates at 700°C, 725°C, and 750°C.

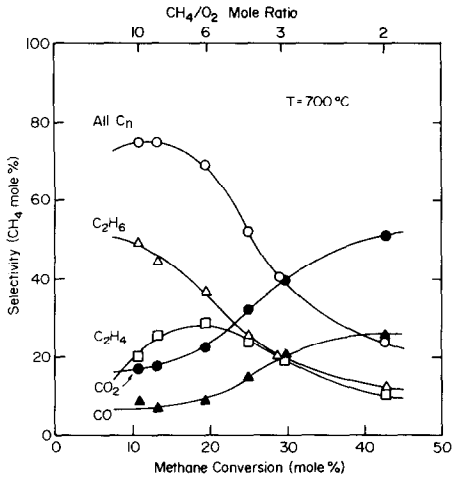

FIG. 10. The dependence of the product selectivity upon methane conversion and CH_4/O_2 mole ratio at 700°C, 0.095 atm O_2, and a gas hourly space velocity of 8×10^5 hr^{-1} (NTP).

The orders of reaction for methane and oxygen were not determined in this study. However, a rough indication of the effects of the partial pressures of methane and oxygen is provided in Fig. 10. In this experiment, the pressure of methane is decreased, while holding the pressure of oxygen and the space velocity constant. At high ratios of oxygen to methane the hydrocarbon products as well as the methane are increasingly converted into CO and CO_2. Throughout the shift in product distribution from C_2 hydrocarbons to carbon oxides, the molar ratio of CO to CO_2 remains constant at 2.0.

The dependence of the product selectivity upon oxygen conversion for ethane reaction over 1 wt% Sr/La_2O_3 is presented in Fig. 11. These data were obtained by varying the residence time at a fixed ratio of C_2H_6 to O_2 of 10/1. The results show that at low conversions substantial amounts of CO, CO_2, and C_2H_4 are produced. As the contact time and O_2 conversion increase, there is a large increase in the selectivity to C_2H_4 relative to CO and CO_2. Since the ratio of ethane to oxygen consumed also increases at longer residence times, this trend can be explained by a greater fraction of the ethylene being produced by nonoxidative dehydrogenation of ethane.

DISCUSSION

On the basis of the dependencies of reactant and product formation on residence time, the following reaction network can be formulated:

Low Conversion

$$CH_4 + (1 - x)/4O_2 \rightarrow \tfrac{1}{2}C_2H_6 + (1 - x)/2H_2O + x/2H_2$$

$$C_2H_6 + (1 - x)/2O_2 \rightarrow C_2H_4 + (1 - x)H_2O + xH_2$$

$$CH_4 + (3 - x)/2O_2 \rightarrow CO + (2 - x)H_2O + xH_2$$

$$CO + \tfrac{1}{2}O_2 \rightarrow CO_2$$

$$CO + H_2O \rightleftarrows CO_2 + H_2$$

High Conversion

$$C_2H_6 + mO_2 \rightarrow CO, CO_2, \text{ and } H_2O$$

$$C_2H_4 + nO_2 \rightarrow CO, CO_2, \text{ and } H_2O$$

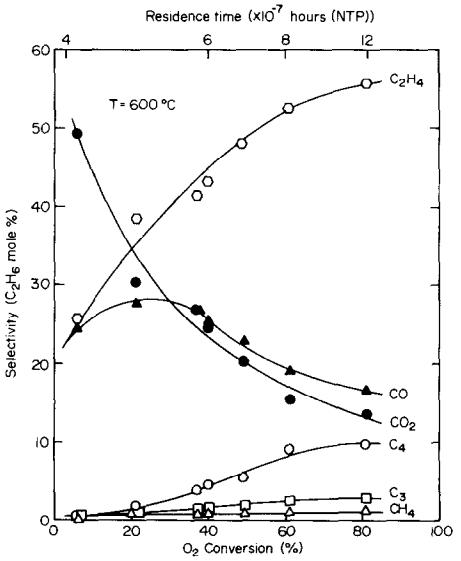

FIG. 11. The dependence of product selectivity upon oxygen conversion and residence time for the reaction of ethane and oxygen at 600°C, 0.46 atm C_2H_6, 0.045 atm O_2, and 0.50 atm argon.

Most of the features of this reaction network are in accord with the literature. All researchers agree that ethane is a primary product of methane activation, and ethylene is formed by dehydrogenation of ethane (*5, 6, 9, 15, 16, 23, 24*). The conversion of ethane into ethylene can occur either oxidatively on the catalyst surface (*5, 6, 15*) or nonoxidatively on the catalyst surface and in the gas phase (*5, 6, 15, 16, 23*). Our results show that the latter reaction dominates both at high oxygen conversions (Fig. 11) and at temperatures greater than 750°C (unpublished work).

However, there is some disagreement over the pathway for generating CO and CO_2 during the oxidative coupling of methane. Sofranko *et al.* (*6*) claim that CO and CO_2 are formed only from the oxidation of ethylene. Many of the other researchers (*5, 15, 16, 23*) report that CO and CO_2 are formed from methane as well as the higher hydrocarbon products. The results of Fig. 8 show that over 1 wt% Sr/La_2O_3, CO and CO_2 taken together are primary products of methane activation. Figure 7 further suggests that CO_2 may be formed by the oxidation of CO. However, this result must be viewed as tentative, because of the high concentration of CO_2 relative to CO, and the competing influence of the water gas shift equilibrium.

At high conversions of O_2 and low ratios of methane to oxygen, the C_2 hydrocarbons can further oxidize to CO and CO_2. The results presented in Fig. 10 indicate that at 700°C and a CH_4/O_2 ratio less than 10, both C_2H_6 and C_2H_4 react with O_2 to form CO and CO_2. Labinger and Ott (*5*) and Sofranko *et al.* (*6*) observed that only ethylene reacted to form CO and CO_2 over a supported manganese oxide catalyst at 825 and 800°C. At these higher reaction temperatures, the rate of C_2H_6 dehydrogenation becomes much faster than the rate of C_2H_6 oxidation, such that the latter reaction is less significant. In addition, the cyclic method of feeding O_2 and CH_4 used by Labinger and Sofranko may have further reduced the rate of C_2H_6 oxidation relative to C_2H_6 dehydrogenation. The increasing rate of oxidation of ethane and ethylene at relatively high O_2 partial pressures limits the yield of coupled hydrocarbons that can be obtained per pass.

Our results indicate that the water gas shift equilibrium influences the carbon oxide product distribution. Evidence for the equilibrium is given by the decrease in CO formation rate with increasing temperature (Fig. 6) and the constant ratio of H_2 to CO in the product (Fig. 9). At 727°C the equilibrium constant for the water gas shift, as written above, is 1.37 (*36*). The ratio of the product concentrations, CO_2 and H_2, to the reactant concentrations, CO and H_2O, observed at 725°C is 0.38. This ratio changed less than 10% over the change in product distribution which occurred with residence time. The ratio of products to reactants is much smaller than the equilibrium constant, suggesting that the water gas shift reaction proceeds part way to equilibrium at the high space velocities employed.

In Table 1, a comparison is made between the apparent activation energies obtained in different studies of the oxidative coupling of methane. A broad range of values has been reported. The methane activation energies observed by us over 1 wt% Sr/La_2O_3, by Otsuka and Jinno (*24*) over Sm_2O_3, and by Kimble and Kolts (*16*) over 1 wt% Li/CaO are in fairly good agreement. However, those of Labinger and Ott (*5*) over Mn/MgO and Ito *et al.* (*15*) over 7 wt% Li/MgO are much higher than the others. We do not know why there are such large differences in the reported values. It is possible that the reaction mechanism could vary depending on the catalyst composition and reaction conditions studied. However, it should be noted that widely differing techniques were used to obtain the Arrhenius relationships. For example, we obtained our rates from the linear dependence of methane conversion upon residence time over a temperature range of 700 to 750°C. On the other hand, Otsuka and

TABLE 1

Comparison of Apparent Activation Energies with Literature Values

Reference	Catalyst	Apparent activation energy (kcal/mole)			Temperature range (°C)
		CH_4	C_2H_6	CO_x	
This work	1 wt% Sr/La_2O_3	39.4	36.8	23.9	700–750
(5)	Mn/MgO	58.0	—	—	750–850
(9)	34 wt% PbO/Al_2O_3	—	23.7	12.2	650–700
(15)	7 wt% Li/MgO	55.2	—	—	560–660
(16)	1 wt% Li/CaO	41.8	—	—	610–770
(23, 24)	Sm_2O_3	35.6	32.3	15.8	600–750

Note. 1 kcal = 4.184 kJ.

Jinno (*24*) abstracted rate constants from a Langmuir–Hinshelwood kinetic model of the reaction over a temperature range of 600 to 750°C.

The mechanism that has been proposed for the oxidative coupling of methane is as follows (*5, 6, 15, 16, 23*): A hydrogen atom is abstracted from methane on the surface of the catalyst, forming a gas-phase methyl radical and a surface hydroxyl group. Methyl radicals in the gas phase combine to form ethane. The methyl radicals also react with oxygen either on the surface or in the gas phase to form CO and CO_2. Ethylene can be formed from ethane several ways: thermal cracking in the gas phase, reaction with methyl radical in the gas phase, reaction with O_2 in the gas phase, and reaction with O_2 on the catalyst surface. The adsorbed hydrogen formed upon methane activation is removed by reaction with oxygen. Kimble and Kolts (*16*) and Labinger and Ott (*5*) have successfully modeled the reaction kinetics by combining the empirical rate of methyl radical formation with the known kinetics of gas-phase reactions of C_1–C_3 hydrocarbons and radicals.

The data we have obtained for the apparent activation energies for ethane and CO_x formation can shed light on the mechanism by which the carbon oxides are formed. As discussed above, ethane is formed by the recombination of methyl radicals in the gas, while CO_x is formed by the reaction of methyl radicals with O_2 either in the gas or on the catalyst surface. Since the activation energy for methyl radical recombination is near zero (*26*), the overall activation energy for ethane formation must equal the overall activation energy for forming gas-phase methyl radicals, E_{CH_3}. Thus, $E_{CH_3} = E_{C_2H_6} = 36.8$ kcal/mole. If CO_x is formed by the gas-phase reaction of methyl radicals and O_2, then the overall activation energy for CO_x formation from methane must at a minimum equal the energy for generating the methyl radicals. However, the apparent activation energy for CO_x formation is 23.9 kcal/mole, substantially less than E_{CH_3}. It is concluded, therefore, that over 1 wt% Sr/La_2O_3 the CO_x is not formed in the gas but on the catalyst surface. In the latter case the apparent activation energy includes terms for the surface reaction, the heats of adsorption of methane and oxygen, and the desorption energy of CO. These terms could combine to give the lower value observed.

The different pathways for generating C_2H_6 and CO_x from CH_4 suggest a means of improving the selectivity to coupled hydrocarbons. It might be possible to selectively poison the catalyst surface for adsorption of O_2 and prevent its reaction with adsorbed

methyl radical. By inhibiting the rate of reaction of adsorbed CH_3 with O_2, a greater proportion of CH_3 radicals with desorb into the gas phase, where they can couple to form ethane. In preliminary experiments it has been found that the selectivity to coupled hydrocarbons can be improved by addition of CO_2. For example, at 750°C, 90 cm^3/min O_2, 750 cm^3/min CH_4, and a catalyst bed volume of 0.32 cm^3, the total hydrocarbon selectivity increased from 58.8 to 74.0 to 91.4% as the CO_2 feed rate increased from 0 to 50 to 100 cm^3/min, respectively. However, the methane conversion decreased at the same time, so that the yield of hydrocarbon products remained relatively constant.

CONCLUSIONS

The results obtained in this study have further defined the reaction network for the oxidative coupling of methane. Methane reacts to form ethane and carbon monoxide. Ethane is favored at high reaction temperatures and low pressures of O_2. Ethane reacts to form ethylene, carbon monoxide, and carbon dioxide. Ethylene, like ethane, is favored at high reaction temperatures and low pressures of O_2. Ethylene will also oxidize to form CO_x at high O_2 pressures. The distribution of CO, CO_2, H_2, and H_2O in the product is largely determined by the water gas shift equilibrium.

REFERENCES

1. Pitchai, R., and Klier, K., *Catal. Rev. Sci. Eng.* **28,** 13 (1986).
2. Scurrell, M. S., *Appl. Catal.* **32,** 1 (1987).
3. Keller, G. E., and Bhasin, M. M., *J. Catal.* **73,** 9 (1982).
4. Labinger, J. A., Ott, K. C., Mehta, S., Rockstad, H. K., and Zoumalan, S., *J. Chem. Soc. Chem. Commun.*, 543 (1987).
5. Labinger, J. A., and Ott, K. C., *J. Phys. Chem.* **91,** 2682 (1987).
6. Sofranko, J. A., Leonard, J. J., and Jones, C. A., *J. Catal.* **103,** 302 (1987).
7. Jones, C. A., Leonard, J. J., and Sofranko, J. A., *J. Catal.* **103,** 311 (1987).
8. Hinsen, W., and Baerns, M., *Chem. Ztg.* **107,** 223 (1983).
9. Hinsen, W., Bytyn, W., and Baerns, M., "Proceedings, 8th International Congress on Catalysis, Berlin, 1984," Vol. 3, p. 581. Dechema, Frankfurt-am-Main, 1984.
10. Bytyn, W., and Baerns, M., *Appl. Catal.* **28,** 199 (1986).
11. Otsuka, K., Yokoyama, S., and Morikawa, A., *Chem. Lett.*, 319 (1985).
12. Ali Emesh, I. T., and Amenomiya, Y., *J. Phys. Chem.* **90,** 4785 (1986).
13. Asami, K., Hashimoto, S., Shikada, T., Fujimoto, K., and Tominaga, H., *Chem. Lett.*, 1233 (1986).
14. Ito, T., and Lunsford, J. H., *Nature (London)* **314,** 721 (1985).
15. Ito, T., Wang, J. X., Lin, C. H., and Lunsford, J. H., *J. Amer. Chem. Soc.* **107,** 5062 (1985).
16. Kimble, J. B., and Kolts, J. H., *Energy Prog.* **6,** 226 (1986).
17. Aika, K., Moriyama, T., Takasaki, N., and Iwamatsu, E., *J. Chem. Soc. Chem. Commun.*, 1210 (1986).
18. Iwamatsu, E., Moriyama, T., Takasaki, N., and Aika, K., *J. Chem. Soc. Chem. Commun.*, 19 (1987).
19. Moriyama, T., Takasaki, N., Iwamatsu, E., and Aika, K., *Chem. Lett.*, 1165 (1986).
20. Yamagata, N., Tanaka, K., Sasaki, S., and Okazaki, S., *Chem. Lett.*, 81 (1987).
21. Deboy, J. M., and Hicks, R. F., *Ind. Eng. Chem. Res.*, in press.
22. Otsuka, K., Jinno, K., and Morikawa, A., *Chem. Lett.*, 499 (1985).
23. Otsuka, K., Jinno, K., and Morikawa, A., *J. Catal.* **100,** 353 (1986).
24. Otsuka, K., and Jinno, K., *Inorg. Chem. Acta.* **121,** 237 (1986).
25. Otsuka, K., and Komatsu, T., *Chem. Lett.*, 483 (1987).
26. Lin, C. H., Cambell, K. D., Wang, J. X., and Lunsford, J. H., *J. Phys. Chem.* **91,** 2682 (1987).
27. Imai, H., and Tagawa, T., *J. Chem. Soc. Chem. Commun.*, 52 (1986).
28. Otsuka, K., Liu, Q., Hatano, M., and Morikawa, A., *Chem. Lett.*, 467 (1986).
29. Otsuka, K., Liu, Q., Hatano, M., and Morikawa, A., *Chem. Lett.*, 903 (1986).
30. Otsuka, K., Liu, Q., and Morikawa, A., *J. Chem. Soc. Chem. Commun.*, 586 (1986).
31. Otsuka, K., Liu, Q., and Morikawa, A., *Inorg. Chem. Acta.* **118,** L23 (1986).
32. Otsuka, K., and Komatsu, T., *J. Chem. Soc. Chem. Commun.*, 388 (1987).
33. Matsuura, I., Utsumi, Y., Nakai, M., and Doi, T., *Chem. Lett.*, 1981 (1986).
34. Matsuura, I., Doi, T., and Utsumi, T., *Chem. Lett.*, 1473 (1987).
35. Deboy, J. M., and Hicks, R. F., *J. Chem. Soc. Chem. Commun.*, in press.
36. Stull, D. R., Westrum, E. F., and Sinke, G. C., "The Chemical Thermodynamics of Organic Compounds." Wiley, New York, 1967.